The use of a temperature-dependent exchange coupling retains the correlation of the cluster with its environment at temperatures above the order-disorder transition. This feature makes it particularly useful in studying the growth of short-range order in a system as the ordering temperature is approached from above.

Below the ordering temperature the theory needs considerable improvement. The magnetization curve is predicted to be a step function, and currently there is no adequate auxiliary relation between long- and short-range correlation functions. It is hoped that the first defect may be remedied by including more of the terms appearing in the general derivation of the cluster Hamiltonian, and that the second need can be filled by studying low-temperature expansions for the correlation functions. At present there seems to be no possibility for extending the theory to include the presence of an external magnetic field.

Since the primary strength of effective field theories is in the temperature region below the ordering transition, and the S.C.C.M. has its greatest effectivenes-above the transition, it is natural to suggest the possis bility of a cluster theory which would include both an effective field and an effective coupling. This would probably involve a self-consistency requirement for both the spin-average and the spin-spin correlation function, which it is hoped would not be too intractable mathematically.

ACKNOWLEDGMENTS

The author is deeply grateful to Professor G. W. Pratt for stimulating his interest in this problem and for many profitable discussions on various aspects of this work. The support of the Office of Naval Research during a major part of this work is also much appreciated.

PHYSICAL REVIEW VOLUME 137, NUMBER 4A 15 FEBRUARY 1965

Second-Harmonic Generation of Light with Double Refraction

G. D. Boyd, A. Ashkin, J. M. Dziedzic, and D. A. Kleinman
Bell Telephone Laboratories, Murray Hill, New Jersey
(Received 27 August 1964)

Experimental and theoretical investigations are reported on the second-harmonic generation (SHG) of light in crystals long enough so that SHG is limited by double refraction. This effect has been called the aperture effect. SHG has been observed in ammonium dihydrogen phosphate (ADP) under matching conditions using the highly parallel beam from a gas laser. Crystals of lengths 5 and 10 cm were used. It was observed that the peak of the SHG is displaced from the peak of the fundamental by a few millimeters. This is the order of magnitude to be expected, since the fundamental is an ordinary ray and the SHG is an extraordinary ray. Since the position of the SHG peak should depend upon absorption, the absorption coefficients of ADP for the fundamental ($\lambda_1=1.1526\,\mu$) and the second harmonic ($\lambda_2=0.5763\,\mu$) were measured and found to be $\alpha_1=0.151$ cm^{-1}, $\alpha_2=0.024$ cm^{-1}; the latter value may represent small-angle scattering rather than true absorption. The matching angle, the angle between the beam and the optic axis for index matching, was measured and found to be $\theta_m=42.7°$. Two kinds of theory are presented. The experiments are first discussed in terms of a heuristic theory which relies upon intuition and plausible physical arguments. The experiments are shown to be in quantitative agreement with this theory. A formal theory is also given for SHG under matching conditions by beams of finite aperture taking into account double refraction and absorption. For parallel beams this theory reduces to the heuristic theory.

1. INTRODUCTION

In this paper we discuss theory and experiments relating to the second-harmonic generation of light (SHG) in very long crystals under index-matching conditions. In particular the limitations imposed by double refraction and absorption will be treated in detail. The experiments are an extension of those undertaken by Ashkin, Boyd, and Dziedzic[1] (ABD) to measure the second-order polarization coefficient d_{36} of potassium dihydrogen phosphate (KDP). In these earlier experiments SHG in a KDP crystal 1.23 cm long was observed from the 1.1526-μ He-Ne optical maser in single-mode operation.

The theory of SHG under matching or nearly matching conditions has been discussed by Kleinman,[2] who defines an effective coherence length due to beam divergence $\ell_{\rm coh}'$ (in this paper labeled ℓ_c' for brevity), which varies inversely as the angular divergence of the beam. Physically, the significance of ℓ_c' is that for thin crystals $\ell<\ell_c'$ the divergence can be neglected, the whole beam can be considered to be matched in phase with the second harmonic light, and SHG varies with thickness as ℓ^2; on the other hand, for long crystals $\ell>\ell_c'$ the divergence of the fundamental beam causes

[1] A. Ashkin, G. D. Boyd, and J. M. Dziedzic, Phys. Rev. Letters **11**, 14 (1963).

[2] D. A. Kleinman, Phys. Rev. **128**, 1761 (1962).

part of it to be mismatched with the second harmonic light and SHG varies as ℓ. Typically for the ruby laser and other solid state lasers $\ell_c' \approx 0.1$ cm owing to many-mode operation and crystal nonuniformities. The success of ABD[1] in observing SHG with the gas maser was due to the very long coherence length ($\ell_c' \sim 10$ cm) possible with the gas maser in single-mode operation.

In the formal treatments of the theory, Armstrong, Bloembergen, Ducuing, and Pershan[3] (ABDP) and Kleinman[2] have represented the laser and second harmonic light by unbounded plane waves. ABDP[3] point out that the interaction between light waves of finite aperture takes place along the direction of energy flow. Kleinman[2] has described SHG in very long crystals in somewhat more detail, pointing out that SHG will ultimately be limited by the slightly different directions of propagation of the energy of the laser and second harmonic beams. This effect, which he has called the *aperture effect*, can be characterized by a length ℓ_a representing the crystal thickness at which a second harmonic beam starting at the incident surface with the same aperture as the laser beam would just separate from the laser beam. The statement is made that regardless of how parallel the laser beam is, the effective coherence length can never be greater than the aperture length ℓ_a, which typically may be of order $\ell_a \sim 10$ cm.

In this paper we report the first observation of the aperture effect. We observe in ammonium dihydrogen phosphate (ADP) crystals of length $\ell = 5.03$ cm and $\ell = 10.4$ cm with an essentially parallel fundamental beam that the peak of the second harmonic intensity is displaced a few millimeters from the peak of the fundamental intensity. Experimentally the effect is quite similar to *double refraction* in birefringent crystals, in which a beam of light breaks up in the crystal into an ordinary and extraordinary ray which propagate in different directions. Since double refraction is already a familiar phenomenon and a familiar term in physics, we shall employ it hereafter as a preferable alternative to the relatively unfamiliar *aperture effect.*

In order to interpret the experimental results, the theory of SHG will be extended to include double refraction, and will be shown to be in substantial agreement with experiment. We emphasize, however, that these developments are natural extensions of the foundations already laid. Two approaches to the theory will be described, each of which is important and useful in its own way. The first, which we call the *heuristic* approach, leans heavily upon plausible and intuitive arguments and is therefore quite easy to follow if one overlooks the complexity of some of the formulas that come out of it. The results obtained by the heuristic theory are correct. The second, or *formal*, approach we consider to be rigorous in that it rests squarely upon the accepted and well-verified theory[2–4] of SHG by unbounded plane waves. To obtain the effects of double refraction it is necessary to represent the finite laser and second harmonic beams as Fourier integrals over plane-wave components. By means of this theory we verify the correctness of the heuristic theory, which we expect will find important applications in cases too complicated to treat formally. We find both experimentally and theoretically that the displacement of the second-harmonic peak intensity depends upon the relative absorptions of the laser and second-harmonic beams.

The role played by diffraction in SHG has not been at all clear up to now. It has been suggested[1,2] that since diffraction causes a divergence of the beam, it can be treated simply by assigning an appropriate coherence length ℓ_c' to take account of the spreading. This cannot be correct, however, since ℓ_c' has been defined[2] in terms of an average over directions of the second harmonic *intensity*, it being assumed that the components in different directions are uncorrelated. Such a description is appropriate if the divergence of the laser beam is due to the presence of many transverse modes. It should also be pointed out that ℓ_c' only takes into account the departure from matching of an uncorrelated diverging beam; it does not take into account the reduction of intensity that accompanies the diverging of the beam. Therefore, the theory of SHG by diverging beams given in Ref. 2 only applies to uncorrelated beams in crystals thin compared to the beam aperture divided by the angular divergence.

In this paper, we are concerned with the case where the laser beam is in a single mode of the optical maser resonator and is therefore completely correlated. The properties of these modes are known in detail from the general theory of the modes in optical resonators.[5–7] When one reflector is spherical and the other is plane with a small transmission, the beam emerging through the plane mirror is extremely parallel for a considerable distance called the *near-field* region, and then diverges in the *far-field* region, making a half cone angle δ_0 equal to $\lambda_1/\pi w_0$, where λ_1 is the fundamental wavelength and w_0 the bean radius to be defined in Sec. 2. This is similar to a plane wave diffracted by an opening of aperture πw_0. For this reason we use the term *diffraction* to refer to that divergence which is characteristic of the modes of the electromagnetic field. The Fourier integral representation of the laser and second harmonic fields may be regarded as an average over directions of the amplitudes of the plane-wave components rather than the intensities. Although the theory of the diffraction effect is considerably more elaborate than the old theory of the divergence effect,[2] it is interesting that ℓ_c' calculated in the old way with the divergence angle δ_0 turns out to be just the aperture length ℓ_a. A full treat-

[3] J. A. Armstrong, N. Bloembergen, J. Ducuing, and P. S. Pershan, Phys. Rev. **127**, 1918 (1962).
[4] N. Bloembergen and P. S. Pershan, Phys. Rev. **128**, 606 (1962).
[5] G. D. Boyd and J. P. Gordon, Bell System Tech. J. **40**, 489 (1961).
[6] G. D. Boyd and H. Kogelnik, Bell System Tech. J. **41**, 1347 (1962).
[7] A. G. Fox and T. Li, Bell System Tech. J. **40**, 453 (1961).

ment of diffraction will be given separately based upon the formal theory introduced here. In this paper we shall only treat in detail the case of the near field.

2. DESCRIPTION OF THE EXPERIMENT

The experimental setup shown schematically in Fig. 1 was arranged to permit direct comparison of the positions of the harmonic beam relative to the fundamental beam at the output face of the long ADP crystals used. In most respects this arrangement is similar to the one used in previous work.[1] The dc excited He-Ne laser with Brewster angle windows was used to produce about 1 mW of polarized cw radiation at 1.1526 μ.

The output was taken through the flat mirror of the half-nonconfocal resonator[5,6] which allows the sample to be placed in the *near field* of the various possible transverse modes of the resonator. Simple iris adjustments serve to select the lowest order transverse mode. For simplicity the present measurements were restricted to the fundamental TEM_{00q} mode which has a Gaussian electric-field distribution and minimum diffraction effects. q is the longitudinal mode number, i.e., the number of half-wavelengths between the reflectors. With a scanning Fabry–Perot interferometer similar to that described by Herriott[8] it was determined that there were three strong longitudinal modes.

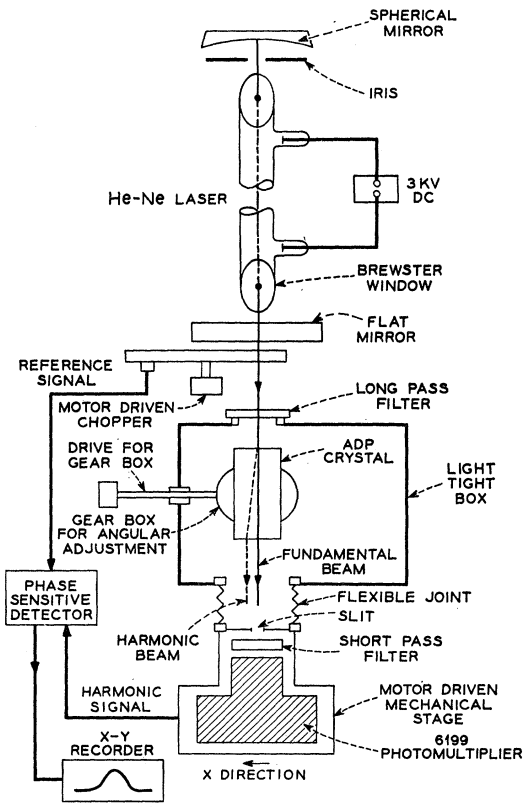

FIG. 1. Schematic diagram of experimental equipment.

[8] D. R. Herriott, Appl. Opt. 2, 865 (1963).

TABLE I. Parameters of the maser beam in free space. The resonator spacing was $d/2=140$ cm, and Δ is evaluated at $z=38$ cm. Aperture length is defined in (3.41).

b' (m)	b (m)	w_0 (cm)	δ_0 (deg)	Δ (deg)	ℓ_a (cm)
50	16.50	0.174	1.21×10^{-2}	0.056×10^{-2}	10.28
10	6.94	0.113	1.86×10^{-2}	0.203×10^{-2}	6.67
3	2.99	0.074	2.84×10^{-2}	0.698×10^{-2}	4.38

According to theory the radial distribution of electric field of the fundamental mode is[5]

$$|E_1(r)|=E_0e^{-r^2/w^2}/(1+\xi^2)^{1/2}, \tag{2.1}$$

where E_0 is a constant. The radial and longitudinal intensity distribution is given by (neglecting absorption)

$$S_1(r)=S_0e^{-2r^2/w^2}/(1+\xi^2). \tag{2.2}$$

The variation of the spot radius w with distance z from the flat mirror is given by

$$w=w_0(1+\xi^2)^{1/2}, \tag{2.3}$$

where

$$\xi=2z/b \tag{2.4}$$

and

$$w_0=(b/k_1)^{1/2}=(b\lambda_1/2\pi n_1)^{1/2} \tag{2.5}$$

is the (minimum) spot size. b is called the *confocal parameter*, the radius and separation of the hypothetical equivalent confocal resonator. λ_1 is the wavelength of the fundamental in free space and n_1 is the refractive index, which in free space is unity. The actual reflectors coincide with the surfaces of constant phase of the hypothetical resonator.

In terms of the radius of curvature b' of the curved reflector and the distance $d/2$ between the two reflectors

$$b=(2b'd-d^2)^{1/2}. \tag{2.6}$$

Defining the beam half-angle at $r=w$ by $\Delta=dw/dz$, one finds

$$\Delta=\delta_0\xi/(1+\xi^2)^{1/2}, \tag{2.7}$$

where

$$\delta_0=\frac{2w_0}{b}=\frac{\lambda_1}{\pi w_0 n_1}=\frac{2}{k_1w_0} \tag{2.8}$$

is the far field diffraction half-angle. When the sample is placed in the *near field* $\xi\ll1$, the effect of the refractive index is to change the far-field diffraction angle according to (2.8) while the spot size remains the same. In the near field the beam is nearly parallel and $\Delta\approx0$, while in the far field $\Delta\approx\delta_0$.

To vary the spot size w_0 mirrors of three different curvatures were used. Table I summarizes the relevant beam parameters at the position of the samples in the near field; namely, 38 cm from the output flat mirror. The aperture length ℓ_a will be defined later.

The linearly polarized fundamental beam from the gas maser is introduced through a long pass filter into a

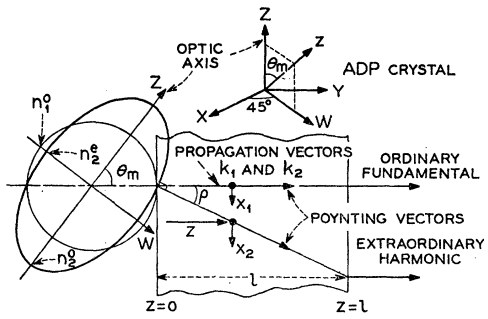

FIG. 2. Illustrating double refraction in SHG. Fundamental enters on the left where we show the index surfaces for the case where the surface normal is a matching direction. The propagation plane ZW containing the optic axis and the beam axis makes an angle of 45° with crystallographic X and Y axes.

light-tight box where it interacts with the ammonium dihydrogen phosphate (ADP) sample as shown in Fig. 1. A 7200:1 gear reduction box permits the angle between the beam and the optic axis to be varied very slowly about the phase matching direction. The extraordinary wave harmonic light generated in the crystal emerges displaced relative to the ordinary wave fundamental as shown schematically in Figs. 1 and 2. Scanning of the fundamental and harmonic beam shapes is accomplished, with the crystal in place, by the transverse motion in the x direction of a detector consisting of a slit perpendicular to the optic axis of the ADP and a short pass filter in front of a RCA 6199 photomultiplier. The narrow slit was used rather than a pinhole in order to get increased signal. There was no loss in resolution inasmuch as the y intensity distribution is known to be Gaussian. Detection with good signal-to-noise ratios involved the use of a 390-cps chopping wheel with a phase-sensitive detector. A simple motor drive on the scanning slit permitted direct recording of the beam shapes on a chart recorder.

The relevant optical properties of ADP are summarized in Table II, and the optical aspects of the experiment are shown schematically in Fig. 2. The matching angle θ_m is given by the expression

$$\sin^2\theta_m=\left(\frac{n_2^e}{n_1^o}\right)^2\frac{[(n_2^o)^2-(n_1^o)^2]}{[(n_2^o)^2-(n_2^e)^2]}, \tag{2.9}$$

where n_1^o and n_1^e are the ordinary and extraordinary refractive indices for the laser light and n_2^o and n_2^e are the corresponding quantities for the second harmonic light. The matching angle θ_m was carefully measured, and (2.9) was used to compute n_1^o. We also measured the double refraction angle ρ at the second harmonic frequency; the result agreed with that computed from (3.1) within experimental error.

Since absorption plays an important role in the interpretation of the double refraction effect, the values of the absorption coefficient α_1 and α_2 were measured directly on the ADP samples used. As summarized in Table II, it was found that $\alpha_1 \gg \alpha_2$ and that about 80% of the laser beam was absorbed in the longer crystal. Furthermore, for these long samples angular deviations from the matching direction as little as 20 sec of arc resulted in a significant decrease of harmonic power. Thus α_1 had to be carefully measured in a manner which included in the absorption coefficient all scatterings[9] larger than 20 sec. This was accomplished by placing a small aperture detector far enough away that the subtended angle at the sample was reduced to 20 sec. Both samples gave $\alpha_1=0.151$ cm^{-1} where about 15% of this value can be attributed to small angle scattering.

Experimental results on double refraction are included in Figs. 3 and 4. The *experimental* fundamental beam intensity as a function of slit position x is shown (dashed curves) for the three choices of reflector and spot radii summarized in Table I. The heights of these curves are normalized to give the same integrated intensity. The corresponding experimentally determined second-harmonic intensities are also shown (points) as a function of x. It is apparent that the double-refraction effect is more pronounced the longer the sample and the smaller the spot size. The width of the slit is indicated in both figures, showing that in no case was the observed intensity distribution limited by resolution. Further discussion of these results will be postponed until after the next section.

TABLE II. Index of refraction and absorption data for ADP. θ_m, α_1, α_2 from present measurements. n_2^o, n_2^e from Refs. (a), (b), (c). n_1^o calculated from (2.9). n_1^e from n_1^o and Ref. (a). ρ computed from (3.1).

	n^o	n^e	$\ell=5.03$ cm α(cm^{-1})	$\ell=10.4$ cm α(cm^{-1})
$\lambda_1=1.1526\,\mu$	1.503_2	1.463_2	0.151	0.151
$\lambda_2=0.5763\,\mu$	1.524_6	1.479_2	0.018	0.024
		θ_m	ρ	
	Radians	0.745	0.030	
	Degrees	42.7°	1.72°	

[a] Anne Marie Vergnoux, Cahiers Phys. **73**, 41 (1956).
[b] I. C. Gardner, Natl. Bur. Std. (U.S.) Report IV-4/Tp 110613, 1947 (unpublished).
[c] R. O'B. Carpenter, J. Opt. Soc. Am. **40**, 225 (1950).

3. HEURISTIC TREATMENT

3.1 Double Refraction and Absorption

The optical maser beam interacting with the negative uniaxial crystal oriented in the phase matched direction is shown schematically in Fig. 2. The refractive index for the fundamental ordinary wave is independent of the direction of propagation and therefore the index surface[2] is a sphere of radius n_1^o. The second harmonic is an extraordinary wave[10,11] and thus the index surface

[9] W. Kaiser and M. J. Keck, J. Appl. Phys. **33**, 762 (1962).
[10] J. A. Giordmaine, Phys. Rev. Letters **8**, 19 (1962).
[11] P. D. Maker, R. W. Terhune, M. Nisenoff, and C. M. Savage, Phys. Rev. Letters **8**, 21 (1962).

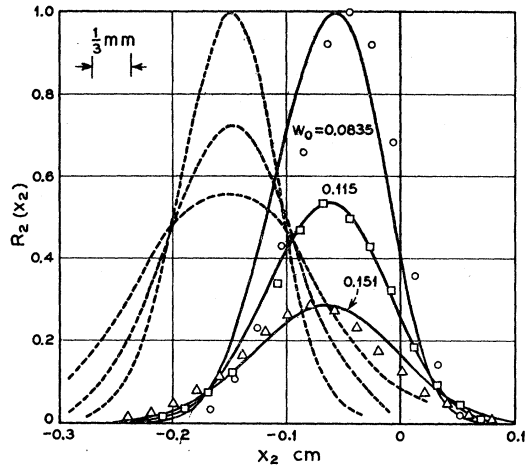

FIG. 3. The slit intensity R_2 of the second harmonic as a function of position x_2. The points are measured values and the curves are calculated from (3.30). Also shown are dashed curves representing the measured fundamental slit intensity. The beam axis is indicated by the peaks of the dashed curves, while the ρ line of Fig. 2 is at $x_2=0$. The crystal length is $l=5.03$ cm.

is an ellipsoid of revolution about the optic axis. The ellipsoid intersects the sphere at the matching angle θ_m and the crystal is so oriented that the optic axis makes an angle θ_m with the surface normal.

It can be shown[12] (see Appendix) that for any direction of *phase propagation* the direction of *energy propagation* (*Poynting vector*) is given by the normal vector to the index surface. For the ordinary wave both vectors are parallel but for the extraordinary wave the Poynting vector deviates from the phase propagation

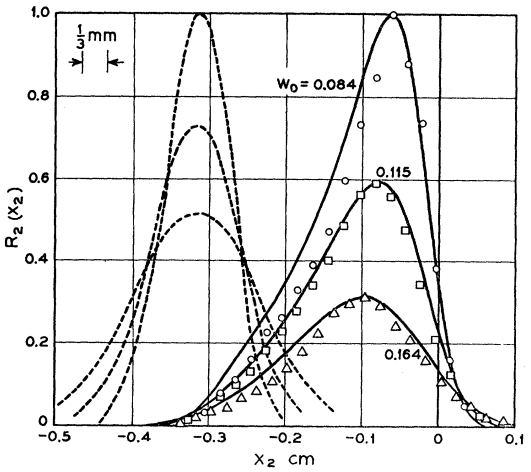

FIG. 4. Same as Fig. 3 for crystal of length $l=10.4$ cm.

[12] H. Kogelnik, H. Motz, *Symposium on Electromagnetic Theory and Antennas, Copenhagen, June 25, 1962* (Pergamon Press Inc., New York, 1963).

direction by an angle ρ given by

$$\tan\rho=\tfrac{1}{2}(n_1^o)^2\left\{\frac{1}{(n_2^e)^2}-\frac{1}{(n_2^o)^2}\right\}\sin 2\theta_m. \qquad (3.1)$$

This angle ρ also governs the usual double-refraction effect (in which both the ordinary and extraordinary waves are at the same frequency), and therefore can be measured directly. The angle ρ in Table II is computed from the index data presented there.

The figure applies to a positive uniaxial crystal if the fundamental is made the extraordinary wave and the second harmonic is made the ordinary wave. The fundamental beam would then follow the ρ line as in ordinary double refraction. The theory to be given here can be carried through in exactly the same way for this case.

For negative uniaxial crystals like ADP or KDP having the point group symmetry $\bar{4}2m(D_{2d},V_d)$ the optimum orientation is that shown in Fig. 2. Define Cartesian coordinates x,y,z such that z is in the propagation direction normal to the surface of the crystal, and the optic axis is in the xz plane. The distinction between the two x coordinates x_1,x_2 will be explained later. The propagation plane (xz) formed by the optic axis and the direction of propagation of the fundamental makes an angle of 45° with the crystallographic X and Y axes. The fundamental is an ordinary wave polarized with the electric vector perpendicular to the plane of the figure (y direction); the second-harmonic polarization is along the optic axis. With this choice of axes the effective component of the polarization transverse to the propagation direction is[1,2]

$$\mathfrak{P}_x=\mathfrak{P}_Z\sin\theta_m=d_{36}E_1^2\sin\theta_m, \qquad (3.2)$$

where d_{36} is the nonlinear coefficient as defined by Kleinman.[2] Here $\mathfrak{P}_x$ and E_1 are wave amplitudes which in general are complex. The second-harmonic polarization will generate a second-harmonic electric field E_2, an extraordinary wave. It has been shown by ABDP[3] that E_2 satisfies the differential equation

$$dE_2/dz=(2\pi i\omega_2/n_1c)\mathfrak{P}_x e^{i(2k_1-k_2)z} \qquad (3.3)$$

where k_1, k_2 are propagation constants ($k_1=2\pi n_1/\lambda_1=\omega_1 n_1/c$) for the fundamental and second-harmonic waves, respectively. In deriving (3.3) it is necessary to assume that both waves are plane waves, although $\mathfrak{P}_x$ may be a slowly varying function of z. We adopt the convention that all wave amplitudes are associated with the time factors $e^{-i\omega_1 t}$ or $e^{-i\omega_2 t}$.

We are particularly concerned here with the special case in which the laser beam is in a *single Gaussian mode*. Near the focus these modes are very much like plane waves except for their finite aperture. It is then appropriate to assume that E_1 is real and write

$$(2\pi\omega_2/n_1c)\mathfrak{P}_x=JS_1, \qquad (3.4)$$

where S_1 is the intensity and

$$J=(16\pi^2\omega_2/n_1^2c^2)d_{36}\sin\theta_m. \tag{3.5}$$

The equation for E_2 now becomes

$$dE_2/dz=iJS_1(z)e^{i(2k_1-k_2)z} \tag{3.6}$$

where we have indicated that S_1 may depend on z in order to include absorption of the laser beam. The integral form of (3.6) giving $E_2(\ell)$ at the exit surface $z=\ell$

$$E_2(\ell)=iJ\int_0^\ell S_1(z)e^{i(2k_1-k_2)z}dz \tag{3.7}$$

has been derived by Franken and Ward[13] by summing the radiation from a phased distribution of dipoles. The absorption of the second harmonic can be accounted for simply by supplying the factor $\exp[-\frac{1}{2}\alpha_2(\ell-z)]$ in the integrand; for the matching case $n_1=n_2$, $k_2=2k_1$ we have

$$E_2(\ell)=iJ\int_0^\ell S_1(z)e^{-\alpha_2(\ell-z)/2}dz. \tag{3.8}$$

Since (3.8) is valid for plane waves it seems plausible that it should also be valid for waves which are nearly plane waves except for being finite in the x,y directions. This leads us to the approximation

$$E_2(x,y,\ell)=iJ\int_0^\ell S_1(x,y,z)e^{-\alpha_2(\ell-z)/2}dz. \tag{3.9}$$

Now refer to Fig. 2; the line at angle ρ, which we shall call the ρ line, represents the direction of energy flow of the second harmonic. Intuitively we should expect that this fact should be taken into account in (3.9); more precisely, we expect that the path of integration should not be along the z direction but along the ρ line. This leads finally to the formula

$$E_2(x,y,\ell)=iJ\int_0^\ell S_1(x-\rho\ell+\rho z,y,z)e^{-\alpha_2(\ell-z)/2}dz, \tag{3.10}$$

which is the basic formula of this section.

In proceeding from (3.3) to (3.10) we have made three assumptions which constitute our *heuristic method*: (a) that E_1 is real, (b) that a finite intensity distribution in the transverse direction can be inserted for $S_1(z)$ in (3.8), and (c) that the path of integration in (3.9) should be along the ρ line. Actually assumption (a) is not at all essential since it could be eliminated simply by writing (3.10) in the slightly more general form

$$E_2(x,y,\ell)=\frac{2\pi i\omega_2}{n_1c}\int_0^\ell \mathfrak{P}_x(x-\rho\ell+\rho z,y,z)e^{-\alpha_2(\ell-z)/2}dz, \tag{3.11}$$

which differs from (3.10) only if the fundamental beam contains more than a single mode. To take mixing of different modes at possibly different frequencies or the spatial mixing of different Fourier components of the same frequency into account it is necessary to use (3.11) with $\mathfrak{P}_x$ given by (3.2) and E_1 expressed as a linear combination of complex field amplitudes representing the modes in the beam.

For convenience later on in discussing the experimental results we shall introduce a new notation for writing (3.10). We denote points in the fundamental beam, the *source* points, by x_1, y_1, z_1, and points in the second-harmonic beam, the *observer* points, by x_2, y_2, z_2. We regard (3.9) as an integral over source points giving the second-harmonic field at an observer point

$$E_2(x_2,y_2,z_2)=iJ\int_0^{z_2} S_1(x_1,y_1,z_1)e^{-\alpha_2(z_2-z_1)/2}dz_1. \tag{3.12}$$

We shall measure the source points from an origin on the beam axis and on the incident surface. Define x_2 for the observer points in such a way that $x_2=0$, $y_2=0$ lies on the ρ line

$$x_2=x-\rho z_2. \tag{3.13}$$

The path of integration over the source points is specified by

$$x_1=x_2+\rho z_1,\quad y_1=y_2=y, \tag{3.14}$$

with x_2 held constant in the integration since it refers to the observer point. Then when we set $z_2=\ell$, (3.12) is identical with (3.10). It should be noted in (3.13) that x_2 measures x coordinates in the second-harmonic beam relative to the ρ line.

We now limit our discussion to SHG under matching conditions in the near field with the laser beam in the fundamental mode. In this case from (2.2)

$$S_1(x_1,y_1,z_1)=S_0e^{-\alpha_1z_1}e^{-2(x_1^2+y_1^2)/w_0^2} \tag{3.15}$$

and (3.12) becomes

$$E_2(x_2,y_2,\ell)=iJS_0e^{-\alpha_2\ell/2}e^{-2y_2^2/w_0^2}\times\int_0^\ell dz_1e^{-\alpha z_1-2(x_2+\rho z_1)^2/w_0^2}, \tag{3.16}$$

where the effective absorption coefficient is

$$\alpha=\alpha_1-\tfrac{1}{2}\alpha_2. \tag{3.17}$$

It is convenient to introduce the normalized variables

$$\begin{aligned} u_1&=\sqrt{2}(x_1/w_0), & u&=\sqrt{2}(x_2/w_0),\\ v&=\sqrt{2}(y_2/w_0), & \tau&=\sqrt{2}(\rho z_1/w_0), \end{aligned} \tag{3.18}$$

and the normalized constants

$$t=\sqrt{2}(\rho\ell/w_0), \tag{3.19}$$

$$q=\alpha w_0/2\sqrt{2}\rho. \tag{3.20}$$

[13] P. A. Franken and J. F. Ward, Rev. Mod. Phys. 35, 23 (1963).

In this notation (3.14) becomes

$$u_1=u+\tau \tag{3.21}$$

and (3.16) may be written

$$E_2(u,v)=iJS_0\ell e^{-(\alpha_2/2)\ell}e^{-v^2}F(u)\,, \tag{3.22}$$

where

$$F(u,t,q)=\frac{1}{t}\int_0^t e^{-2q\tau}e^{-(u+\tau)^2}d\tau\,. \tag{3.23}$$

The function $F(u)$ may be expressed in terms of the error integral

$$\mathrm{erf}x=\frac{2}{\pi^{1/2}}\int_0^x e^{-z^2}dz \tag{3.24}$$

as follows:

$$F(u,t,q)=\frac{\pi^{1/2}}{2t}e^{+q(q+2u)}\{\mathrm{erf}(t+u+q)-\mathrm{erf}(u+q)\}\,. \tag{3.25}$$

The total fundamental power is related to the peak fundamental intensity by

$$P_1=\tfrac{1}{2}\pi w_0^2S_0\,. \tag{3.26}$$

The second-harmonic time-average intensity

$$S_2=\frac{n_2c}{8\pi}E_2E_2^* \tag{3.27}$$

is given by

$$S_2(u,v)=KP_1^2\ell^2e^{-\alpha_2\ell}(4/w_0^4\pi)e^{-2v^2}F(u)^2\,, \tag{3.28}$$

where, with $n_1=n_2$, K is the constant

$$K=\frac{n_1c}{8\pi^2}J^2=\frac{32\pi^2\omega_2^2}{(n_1c)^3}d_{36}^2\sin^2\theta_m \tag{3.29}$$

independent of power, crystal thickness, and beam size.

Since our experiment only measures the intensity distribution in the x direction by means of a moving slit, we must integrate over the y direction; therefore the *slit intensity*

$$R_2(u)=\int_{-\infty}^{+\infty}S_2(u,v)dy=KP_1^2\ell^2e^{-\alpha_2\ell}\frac{2}{w_0^3\pi^{1/2}}F(u)^2 \tag{3.30}$$

is the quantity to be compared with the data of Figs. 3 and 4. The expression takes into account double refraction and absorption but not diffraction, since the spot radius is assumed a constant w_0 throughout the crystal.

Although we have written $F(u)$ for brevity, it is clear from (3.25) that this function also depends on the (normalized) thickness t and (normalized) effective absorption coefficient q. The behavior of $F(u,t,q)^2$ is shown in Figs. 5 and 6. The point labeled 0 on the u axis corresponds to the point in Fig. 2 where the ρ line meets the exit surface, while the point $-t$ corresponds

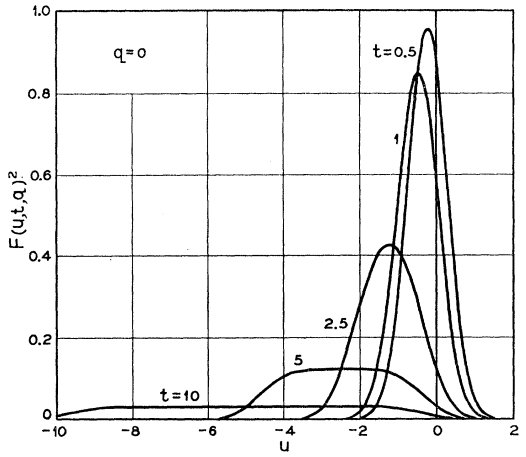

FIG. 5. The function $F(u,t,q)^2$ defined by (3.25) as a function of u for $q=0$ and several values of t.

to the beam axis. If $t\gg1$ the SHG takes place almost entirely in the range $-t<u<0$. If $t<1$ it means that the spot size is so great, or the crystal so thin, that double refraction is obscured. When $t\gg1$ and $q=0$ the curve is very flat in the double-refraction range and rapidly falls to zero outside this range as shown in Fig. 5 for $t=5$ and $t=10$. This is what we should expect to observe in very long crystals $\rho\ell\gg w_0$ with no absorption. We note from (3.17) and (3.20) that it is possible to have $q\sim0$ even in the presence of absorption. When $q>0$ the curve peaks toward the ρ line, and when $q<0$ it peaks toward the beam axis as shown in Fig. 6. This effect can be understood very easily as follows: When $q>0$ the dominant absorption is that of the laser beam, which becomes too weak deep in the crystal for

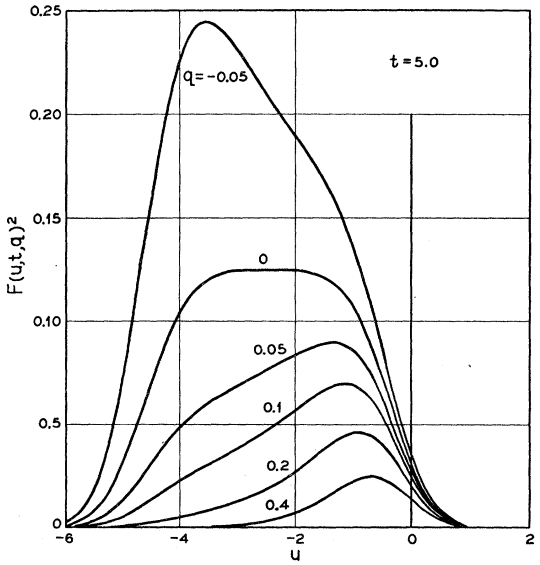

FIG. 6. The function $F(u,t,q)^2$ as a function of u for $t=5.0$ and several values of q.

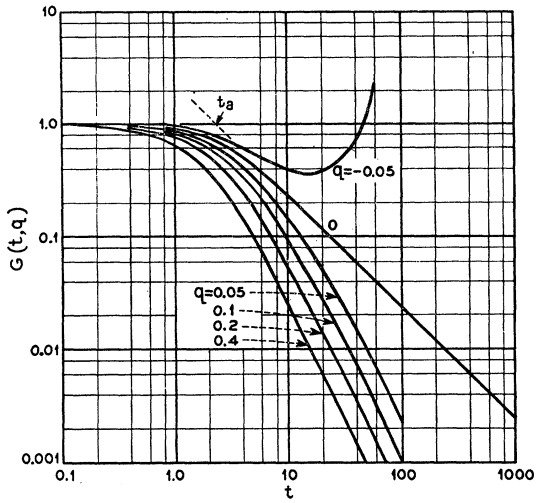

FIG. 7. The function $G(t,q)$ defined in (3.33) as a function of t for several values of q.

significant SHG; the relevant region for SHG is therefore near the incident surface, and the second harmonic energy flows out along the ρ line. On the other hand, when $q<0$ the second harmonic is so strongly absorbed that SHG takes place near the exit surface on the beam axis.

3.2 The Aperture Length

The total SHG power is given by

$$P_2=\int_{-\infty}^{+\infty} R_2(u)dx_2 \tag{3.31}$$

which may be written

$$P_2=KP_1^2\ell^2e^{-\alpha_2\ell}(1/w_0^2)G(t,q)\,, \tag{3.32}$$

where

$$G(t,q)=\left(\frac{2}{\pi}\right)^{1/2}\int_{-\infty}^{+\infty}F(u,t,q)^2du\,,$$
$$G(0,0)=1\,. \tag{3.33}$$

For the purpose of numerical computation it is best to use the form

$$G(t,q)=\frac{\pi^{1/2}}{t^2}e^{-6q^2-2qt}[N(t,q)+N(t,-q)]\,, \tag{3.34}$$

where

$$N(t,q)=e^{-2qt}\int_{c_1}^{c_2}e^{cqx}\,\mathrm{erf}x\,dx \tag{3.35}$$

$$c_1=2q/\sqrt{2}\,,\quad c_2=(t+2q)/\sqrt{2}\,,\quad c=4\sqrt{2}$$

as can be obtained from (3.23) and (3.33) by interchanging the order of integration. The total harmonic power P_2 is seen to be proportional to $G(t,q)$. In the limiting case of a thin nonabsorbing crystal we have $t,\ q\to 0$ and $G\to 1$, and the total power is given by

$$P_2\to KP_1^2\ell^2/w_0^2\,, \tag{3.36}$$

which agrees[14] with Eq. (1) of ABD[1] and Kleinman's[2] equation (123) as expected. Note that P_2 varies as ℓ^2 in this limit which is characteristic of SHG by an unbounded plane wave in the index matching direction.

In the previous discussion[2] of the *aperture effect* it was proposed that there should be a critical length such that in long crystals SHG no longer increases at ℓ^2. That discussion did not state precisely how SHG should vary with ℓ nor describe the field distribution, although it was stated that the field would never grow larger than a certain maximum value. In the case of nonabsorbing thick crystals $t\gg 1$, $q=0$, the intensity distribution has the form

$$\lim_{t\to\infty,\,q\to 0}F(u,t,q)^2=0 \qquad (u<-t)$$
$$=\pi/t^2 \qquad (-t<u<0) \tag{3.37}$$
$$=0 \qquad (u>0)\,.$$

In the case of $q=0$ Eq. (3.35) may be integrated directly; the result is

$$G(t,0)=([2\pi]^{1/2}/t)\,\mathrm{erf}(t/\sqrt{2})-(2/t^2)(1-e^{-t^2/2})\,. \tag{3.38}$$

The function $G(t,q)$ given in (3.33), (3.34), and (3.38) is plotted as a function of t in Fig. 7 for several values of q; for $q\neq 0$ the curves were computed by numerical integration.

For the nonabsorbing case the asymptotic dependence of G can be obtained from (3.38) as

$$\lim_{t\to\infty,\,q\to 0}G(t,q)\to\frac{(2\pi)^{1/2}}{t}=\pi^{1/2}\frac{w_0}{\rho\ell}\,, \tag{3.39}$$

from which a normalized aperture length may be defined

$$t_a=(2\pi)^{1/2}\approx 2.5\,. \tag{3.40}$$

This is the intersection of the asymptotes for $t\to 0$ and $t\to\infty$ when $q=0$. From (3.39) the aperture length is

$$\ell_a=\pi^{1/2}\frac{w_0}{\rho}=1.77\frac{w_0}{\rho}\,. \tag{3.41}$$

For crystals of length $\ell>\ell_a$ the dependence of SHG power P_2 on length changes from quadratic to linear as seen in Fig. 7. The linear dependence of P_2 on ℓ comes about because the second-harmonic intensity reaches a maximum value within the double-refraction region, but the area of this region on the exit surface grows linearly with ℓ.

3.3 The Coherence Length

It is interesting to show how the effect of double refraction on P_2 just derived can be obtained by a

[14] A printer's error exists in Eq. (1) of Ref. (1) in that the ω should be ω^2.

completely different line of argument which ascribes the effect to divergence of the beam and departure from matching. We present this as a curiosity and not as an alternative treatment, since it does not lead to a correct description of the true field distribution. A rigorous treatment of diffraction will be published separately. Following Kleinman[2] we consider only the effect of the divergence on the phase matching and not its effect on the laser intensity, and we regard the laser beam as an uncorrelated bundle of plane waves. Since we now ignore the double refraction effect, we write (3.36) in the form

$$P_2=KP_1^2(\ell^2/w_0^2)\langle(\sin^2\psi)/\psi^2\rangle, \tag{3.42}$$

where

$$2\psi=(2k_1-k_2)\ell \tag{3.43}$$

measures the phase mismatch. We consider that along the beam axis perfect phase matching occurs ($\psi=0$), but away from the axis in the xz plane there is a small mismatch. Consider rays of the fundamental beam as being lines along the propagation vector at each point. Thus the trajectory of a ray is given by

$$r^2=r_0^2(1+\xi^2). \tag{3.44}$$

The special case of $r=w$ is the spot radius at which the electric field falls to e^{-1} of its axial value as given in Eq. (2.3). A ray may be identified by the value of

$$r/w=r_0/w_0. \tag{3.45}$$

At a distance z from the beam minimum, the ray makes an angle with the axis of

$$\delta=\frac{dr}{dz}=\delta_0\frac{r_0}{w_0}\frac{\xi}{(1+\xi^2)^{1/2}}=\frac{r_0}{w_0}\Delta, \tag{3.46}$$

where δ_0 and Δ have been defined in (2.8) and (2.7).

The component of δ seen in the xz plane is the angular deviation from the phase matched direction

$$\delta_x=(x/r)\delta=(x_0/w_0)\Delta. \tag{3.47}$$

The phase mismatch may be written[1,2]

$$\psi=\beta\ell\delta_x, \tag{3.48}$$

where

$$\beta=k_1\sin\rho. \tag{3.49}$$

Define

$$\mathcal{T}=\beta\ell\Delta/\sqrt{2}=t\Delta/\delta_0, \tag{3.50}$$

where t was previously defined by Eq. (3.19). It follows for $\rho\ll1$ that

$$\psi=\mathcal{T}u_1. \tag{3.51}$$

We now average $\sin^2\psi/\psi^2$ over u_1 using as the weighting function the square of the fundamental intensity which varies as $e^{-2u_1^2}$. Since $\mathcal{T}$ depends on ξ or z through the ray angle we face the question of what is the appropriate value to use for $\mathcal{T}$. For the moment, however, consider $\mathcal{T}$ some constant and carry out the average as

$$\frac{\sin^2\psi}{\psi^2}=\left(\frac{2}{\pi}\right)^{1/2}\int_{-\infty}^{+\infty}e^{-2u_1^2}\frac{\sin^2(\mathcal{T}u_1)}{(\mathcal{T}u_1)^2}du_1. \tag{3.52}$$

This may be integrated by the technique of replacing the 2 in the exponential by a dummy variable, differentiating with regard to this variable and integrating over u_1. This result may then be integrated over the dummy variable to obtain the result

$$\frac{\sin^2\psi}{\psi^2}=\frac{(2\pi)^{1/2}}{\mathcal{T}}\operatorname{erf}\left(\frac{\mathcal{T}}{\sqrt{2}}\right)$$
$$-\frac{2}{\mathcal{T}^2}[1-\exp(-\mathcal{T}^2/2)]\to1 \quad \text{for} \quad \mathcal{T}\ll(2\pi)^{1/2}$$
$$\to(2\pi)^{1/2}/\mathcal{T} \quad \text{for} \quad \mathcal{T}\gg(2\pi)^{1/2}. \tag{3.53}$$

This result is identical to that of $G(t,0)$ of Eq. (3.38) shown in Fig. 7 where the variable $\mathcal{T}$ replaces t in that formulation.

If one were to Fourier analyze the fundamental beam, plane-wave components would appear having directions within the entire diffraction cone of half-angle δ_0. The small values of Δ in the near field are therefore irrelevant to the present calculation. It is therefore quite reasonable that the appropriate value of $\mathcal{T}$ is that corresponding to $\Delta=\delta_0$ so (3.50) becomes

$$\mathcal{T}=t. \tag{3.54}$$

We still use the ray picture, however, to derive the linear dependence of ψ upon u_1 in (3.51) and the linear dependence of $\mathcal{T}$ upon ℓ. The critical length at which P_2 stops increasing as ℓ^2 and increases as ℓ is determined by the condition $t=(2\pi)^{1/2}$ just as for double refraction. We emphasize that the divergence of the beam, except for the effect on the intensity not considered here, when the laser beam is in a single mode does not introduce a new effect not already taken into account in double refraction. Furthermore, the effective coherence length ℓ_c' previously defined by Kleinman is identical in this case with the aperture length of Eq. (3.41).

3.4 Position of Maximum Slit Intensity

As an aid in analyzing experimental results it is convenient to have approximate formulas giving the position of the maximum of $F(u)$. From (3.25) the condition $(dF/du)=0$ gives

$$\pi^{1/2}q[\operatorname{erf}(\tfrac{1}{2}t+h)+\operatorname{erf}(\tfrac{1}{2}t-h)]$$
$$=2e^{-h^2}e^{-t^2/4}\sinh(th), \tag{3.55}$$

where

$$h=u+q+\tfrac{1}{2}t \tag{3.56}$$

is a convenient variable for describing the position of the peak. For $q=0$ the solution of (3.55) is $h=0$; for

$h \ll 1$, $h \ll t/2$,

$$h = (1/t)\sinh^{-1}[\pi^{1/2} q \operatorname{erf}(t/2) e^{t^2/4}]. \quad (3.57)$$

If $|ht| \gg 1$ and $\frac{1}{2}t \pm h \gg 1$ the solution of (3.55) is

$$h = \operatorname{sgn}(q)\{\tfrac{1}{2}t - [-\ln(2|q|\pi^{1/2})]^{1/2}\} \quad (3.58)$$

providing $|q| < \frac{1}{2}\pi^{-1/2}$. This formula predicts the peak positions in Figs. 3 and 4 very satisfactorily. If $t > 2$ the domains of validity of (3.57) and (3.58) in q are approximately

$$\begin{aligned} &(3.57) \quad 0 \leq 2\pi^{1/2}|q| < e^{t/2 - t^2/4}, \\ &(3.58) \quad e^{-t^2/4} < 2\pi^{1/2}|q| < 1. \end{aligned} \quad (3.59)$$

We have not devised a convenient formula valid for $|q| > \frac{1}{2}\pi^{-1/2} = 0.28$.

4. DISCUSSION OF EXPERIMENTAL RESULTS

Second-harmonic generation has been studied using three beam spot sizes and two crystal lengths. The experiment was performed by scanning the second harmonic and fundamental beams with a slit. The experimental slit intensities R_1 (dashed curve) and R_2 (points) are shown in Figs. 3 and 4. Also shown are theoretical curves for R_2 calculated from (3.30) and the appropriate experimental parameters.

All of the parameters in the theory are determined from the known values of the thickness ℓ, the spot size w_0, the absorption coefficients α_1, α_2, and the double refraction angle ρ defined by (3.1). The R_1 curves are normalized to constant power P_1, which implies that the peaks of R_1 vary inversely as w_0. The theoretical R_2 curves are also calculated for constant P_1. The experimental R_2 points have been normalized to the *same peak height* as the corresponding theoretical curve to facilitate comparison of the shapes of the theoretical and experimental curves. The measured peaks of R_2 agree closely with theory in their dependence on w_0.

The comparison of theoretical and experimental peak heights is summarized in Table III. For comparing peak heights we define the quantity

$$M(b',50) = \frac{\max[R_2(u)]_{b'}}{\max[R_2(u)]_{b'=50}}. \quad (4.1)$$

The theoretical [calculated from (3.30)] values $M(b',50)_{\text{theor}}$ and experimental values $M(b',50)_{\text{exp}}$ and their ratios are given in Table III.

The total (relative values) second-harmonic power P_2 is given in Table IV as a function of w_0. Also tabulated are the values of t (3.19) and q (3.20) obtained from the measured parameters and used to plot the theoretical curves in Figs. 3 and 4.

It is apparent from Figs. 3 and 4 that theory and experiment are in satisfactory over-all agreement in regard to peak positions and shapes. In Fig. 3 there are minor discrepancies in peak positions for $w_0 = 0.0835$ and 0.151. In Fig. 4 there seems to be a discrepancy in the width of the $w_0 = 0.084$ peak and to a lesser extent the 0.164 peak. We have no explanation for these minor discrepancies. The dependence of second-harmonic power on spot size given in Table IV is also in reasonably good agreement with theory. The greatest discrepancy occurred for $w_0 = 0.084$ in the 10.4-cm crystal. It is difficult to discuss the experimental errors in these experiments. It seems that the discrepancies are not due to the slitwidth or difficulty in measuring the position x_2 of the slit. The most likely source of error is in the measurements of power.

5. FORMAL TREATMENT

5.1 Basic Equations

The theory of SHG by plane polarization waves has been treated in considerable detail. This is a special case of the interaction of three plane waves for which ABDP[3] have given an exact solution. Since we are concerned here with SHG in long crystals, it may be of interest to consider the possibility of the efficient conversion of power from the fundamental to the second-harmonic beam. Under matching conditions with no absorption the fundamental field amplitude $E_1(z)$ and the second-harmonic field amplitude $E_2(z)$ satisfy the

TABLE III. Comparison of theoretical and experimental peak heights. $M(b',50)$ is defined in (4.1).

b' (meters)	w_0(cm) theory	w_0(cm) exp	$M(b',50)_{\text{theor}}$	$M(b',50)_{\text{exp}}$	$\frac{M_{\text{exp}}}{M_{\text{theor}}}$
		$\ell = 5.03$ cm crystal			
50	0.174	0.151	1.0	1.0	1.0
10	0.113	0.115	1.91	1.97	1.03
3	0.074	0.0835	3.57	3.88	1.09
		$\ell = 10.4$ cm crystal			
50	0.174	0.164	1.0	1.0	1.0
10	0.113	0.115	1.89	1.87	0.99
3	0.074	0.084	3.17	4.35	1.37

TABLE IV. Ratio of total SHG power P_2 for various fundamental beam sizes. Normalized parameters t (3.19) and q (3.20) based on experimental spot radius w_0 and parameters of Table II.

b' (meters)	w_0(cm) exp	t	q	P_2 theory	P_2 exp	$\frac{P_{2\,\text{exp}}}{P_{2\,\text{theory}}}$
		$\ell = 5.03$ crystal				
50	0.151	1.41	0.253	1	1	1
10	0.115	1.86	0.192	1.58	1.61	1.02
3	0.0835	2.56	0.140	2.57	2.68	1.04
		$\ell = 10.4$ cm crystal				
50	0.164	2.69	0.269	1	1	1
10	0.115	3.84	0.188	1.60	1.73	1.08
3	0.084	5.25	0.138	2.35	3.40	1.45

relations[3]

$$E_1(z)=E_1(0)\ \mathrm{sech}(z/\ell_p),\qquad E_2(z)=iE_1(0)\ \tanh(z/\ell_p),\tag{5.1}$$

where the characteristic length ℓ_p for power conversion is

$$\ell_p=(cn/2\pi\omega)d^{-1}E_1(0)^{-1},\tag{5.2}$$

with n the refractive index, ω the second-harmonic frequency, and d the appropriate component of the second-order polarization tensor. We estimate that in the present experiments $E_1(0)\sim 0.02$ esu (6 V/cm), and $d=d_{36}\sim 3\times 10^{-9}$ esu, so that (5.2) gives

$$\ell_p\sim 10^5\ \mathrm{cm}.\tag{5.3}$$

Since this is much longer than the crystals we have in mind, and longer than the absorption length of most crystals, we are justified in treating the polarization wave as an externally applied and specified source.

The theory of SHG by unbounded plane polarization waves has been treated by Bloembergen and Pershan[4] and by Kleinman.[2] Under *matching conditions* with no absorption the field amplitude is given by

$$E_2(z)=2\pi i(\omega/cn)dE_1{}^2z,\tag{5.4}$$

where z is measured from the incident surface of the crystal and the beam propagates normal to the surface. This agrees with the second relation (5.1) in the limit $z\ll\ell_p$, and also with (3.3). The linear growth of $E_2(z)$ may be ascribed[2] to constructive interference between a *forced wave* generated by the polarization and a *free wave*, or light wave, generated at the surface by the forced wave. It is equally valid to ascribe the growth to constructive interference between the waves radiated from each differential slab of polarization in the material; according to this view we regard (3.3) as the fundamental equation, and (5.4) is the solution for the matching case satisfying $E_2(0)=0$. Actually (5.4) does not give the entire second-harmonic field. The value of $E_2(0)$ is related to the amplitudes of nongrowing waves in the medium and a reflected wave at the surface.[2-4] These waves are many orders of magnitude weaker than the growing wave (5.4), and may be neglected in the experiments we are considering here.

The theory of SHG is based upon the inhomogeneous vector wave equation[2,3]

$$\nabla\times\nabla\times\mathbf{E}-(\omega/c)^2\epsilon_2\cdot\mathbf{E}=4\pi(\omega/c)^2\mathfrak{P}_K e^{i\mathbf{K}\cdot\mathbf{r}},\tag{5.5}$$

where ϵ_2 is the dielectric constant tensor at the frequency ω, and $\mathbf{K}$ is the wave vector of the polarization wave. If, as in previous treatments, we regard the laser beam as an unbounded plane wave of wave vector $\mathbf{k}_1$, it follows that $\mathbf{K}=2\mathbf{k}_1$. A beam of finite aperture, however, has other Fourier components, and it is our main purpose in this section to take proper account of these and determine their effects. We begin by reviewing briefly the theory as given by Kleinman[2] in the absence of absorption.

The general solution of (5.5) consists of a forced wave (or inhomogeneous wave[3,4]), which is some convenient particular solution of the inhomogeneous equation, and suitable free waves, which are solutions of the homogeneous equation obtained by setting $\mathfrak{P}_K=0$. The free waves are chosen so as to satisfy the boundary conditions of the problem. The free waves have the form

$$E\mathbf{U}e^{i(\omega/c)n_2\mathbf{s}\cdot\mathbf{r}},\tag{5.6}$$

where the refractive index $n_2=n_2(\mathbf{s})$ is a function of the direction $\mathbf{s}$ (unit vector) of the wave vector

$$\mathbf{k}_2=(\omega/c)n_2\mathbf{s}.\tag{5.7}$$

The polarization direction $\mathbf{U}=\mathbf{U}(\mathbf{s})$ (unit vector) is also a function of $\mathbf{s}$ satisfying together with n_2 the relation

$$\alpha_s\cdot\mathbf{U}=0,\tag{5.8}$$

where α_s is the dyadic

$$\alpha_s=n_2{}^2(I-\mathbf{ss})-\epsilon_2,\tag{5.9}$$

with I the unit dyadic or idemfactor. Equations (5.8), and (5.9) determine both n_2 and $\mathbf{U}$. We may define a quantity n', called the effective index, and a unit vector $\boldsymbol{\sigma}$, by the relation

$$\mathbf{K}=(\omega/c)n'\boldsymbol{\sigma}\tag{5.10}$$

similar in form to (5.7). In general $n'\neq n_2(\boldsymbol{\sigma})$, since we are considering the general case of arbitrary $\mathbf{K}$.

When $n'\neq n_2(\boldsymbol{\sigma})$ the polarization wave is said to be *mismatched*; the mismatch is described quantitatively by φ' in the relation

$$n'\boldsymbol{\sigma}-n_2\mathbf{s}=\varphi'\mathbf{N},\tag{5.11}$$

where $\mathbf{N}$ is the direction (unit vector) normal to the incident surface of the crystal. This equation determines both φ' and $\mathbf{s}$ to be associated with a prescribed $n'\boldsymbol{\sigma}$. Here n_2 and $\mathbf{s}$ specify a free wave (5.6) which must exist in the presence of the forced wave in order to satisfy boundary conditions at the surface. It can be shown[2] that if $\varphi'\ll 1$ it is not necessary to specify exactly the boundary conditions or to take into account all of the waves present. The dominant effect is the production of a growing wave through the interference of the forced wave with one free wave. When $\varphi'=0$ the waves are said to be *matched*, and the growing wave is given by (5.4). More generally, under *nearly matching* conditions the growing wave is given by

$$\mathbf{E}_K(\mathbf{r})=\mathbf{N}\cdot\mathbf{r}g(2i\psi_K)\gamma\cdot\mathfrak{P}_K e^{i\mathbf{K}\cdot\mathbf{r}},\tag{5.12}$$

where

$$g(x)=\frac{1-e^{-x}}{x}=\int_0^1 e^{-px}dp\tag{5.13}$$

and

$$2\psi_K=(\omega/c)\varphi\mathbf{N}\cdot\mathbf{r}.\tag{5.14}$$

In general φ in (5.14) is complex, but in the absence of

absorption we have $\varphi=\varphi'$. The dyadic γ is defined by

$$\gamma=-2\pi i(\omega/cn)[(\mathbf{N}\cdot\mathbf{U})(\boldsymbol{\sigma}\cdot\mathbf{U})-\mathbf{N}\cdot\boldsymbol{\sigma}]^{-1}\mathbf{UU}, \quad (5.15)$$

where n and $\mathbf{U}$ refer to the nearly matched free wave. To a good approximation γ can be written

$$\gamma=2\pi i(\omega/cn)\mathbf{UU}, \quad (5.16)$$

providing the laser beam is nearly normal to the surface. Here the dyadic $\mathbf{UU}$ acts as a projection operator to select that component of $\mathfrak{P}$ which is effective in producing a growing second-harmonic wave. For the arrangement considered in Sec. 3, $\gamma\cdot\mathfrak{P}$ is in the x direction and (3.4) could be written

$$(\gamma\cdot\mathfrak{P})_x=iJS_1, \quad (5.17)$$

which establishes the connection between (5.12) and our previous formulas in Sec. 3. For the matching case $g(2i\psi_K)=g(0)=1$ and (5.12) reduces to (5.4). Away from matching, the function $g(2i\psi_K)$ oscillates with distance to give the familiar coherence length effect[11] used in (3.42), $|g(2i\psi)|=|(\sin\psi)/\psi|$.

5.2 Absorption

The essential equations which we need from the previous theory, and which we have quoted without proof, are (5.11) and (5.12). The first generalization which we must make in the theory is to introduce absorption. Absorption of the fundamental may be introduced formally into (5.5) by letting $\mathbf{K}$ be complex. Absorption of the second harmonic corresponds to complex ϵ_2, which leads to a complex refractive index n_2. The usual procedure for isotropic media is to assume light waves of the form (5.6) with complex n_2 which can be expressed in terms of the real and imaginary parts of ϵ_2. This can also be done for anisotropic media, but the relationship of n_2 to ϵ_2 is very much more complicated. Nevertheless, we may consider the theory for unbounded plane waves to be formally complete, since the Fresnel equations for the surface waves[2] (or boundary harmonics[4]) remain formally valid for complex ϵ_2 and $\mathbf{K}$.

It is well known[15] that the use of a complex refractive index leads to complex angles in the Fresnel equations which have no obvious geometrical significance. The complex angles arise because one is requiring the real and imaginary parts of the wave vectors to have the same direction. This is an unnatural requirement because the planes of constant phase do not necessarily coincide with the planes of constant amplitude. It is obvious physically that the amplitude planes, in a medium with a plane incident surface, must be parallel to the surface, whereas the phase planes can have an arbitrary direction. It follows that the complex angles can be eliminated from the theory if the light waves are written in the form

$$E\mathbf{U}e^{i(\omega/c)n_2\mathbf{s}\cdot\mathbf{r}-\alpha_2\mathbf{N}\cdot\mathbf{r}/2}, \quad (5.18)$$

where n_2 and α_2 are real. This corresponds to a complex wave vector

$$\mathbf{k}_2=(\omega/c)n_2\mathbf{s}+\tfrac{1}{2}i\alpha_2\mathbf{N}, \quad (5.19)$$

in which the imaginary part has been given the correct direction from the outset. Similarly, the polarization wave can be written in the form

$$\mathfrak{P}_K e^{i\mathbf{K}\cdot\mathbf{r}-\alpha_1\mathbf{N}\cdot\mathbf{r}} \quad (5.20)$$

with real $\mathbf{K}$ and α_1.

Although it is not necessary to use complex angles, there is a price to pay for the convenience of using real angles having the usual geometrical significance. Strictly speaking, n_2 and α_2 in (5.19) are not characteristic of the medium alone but also depend on the orientation of the surface $\mathbf{N}$. This can be a serious difficulty for large absorption and large deviations from normal incidence. On the other hand, if the absorption is small and the deviations from normal incidence are small, this complication is of no concern. We can regard n_2 and α_2 in (5.19) as the usual refractive index and absorption coefficient. Similarly, α_1 is essentially identical with the ordinary absorption coefficient for the fundamental beam.

In (5.11) we have defined a real function φ' to measure the mismatch in the absence of absorption. In the presence of absorption we must generalize the mismatch function to take into account the imaginary parts of the wave vectors. The general *complex mismatch function* φ must satisfy

$$n'\boldsymbol{\sigma}-n_2\mathbf{s}+i(c/\omega)\alpha\mathbf{N}=\varphi\mathbf{N}, \quad (5.21)$$

where α has already been defined in (3.17). The solution of (5.21) is

$$\varphi=\varphi'+i\varphi'', \quad (5.22)$$

where φ' is given by (5.11) and

$$\varphi''=(c/\omega)\alpha. \quad (5.23)$$

It follows from (5.14) that

$$2\psi_K=(\omega/c)\varphi'\mathbf{N}\cdot\mathbf{r}+i\alpha\mathbf{N}\cdot\mathbf{r}. \quad (5.24)$$

We see that absorption enters the problem in two distinct ways; the absorption of the second harmonic enters through (5.24) where it affects the phase matching, and the absorption of the fundamental enters both through (5.24) and (5.20) representing the attenuation of the polarization wave. Replacing $\mathfrak{P}_K\exp(i\mathbf{K}\cdot\mathbf{r})$ by (5.20) in (5.12) gives the general form for the second-harmonic electric field

$$\mathbf{E}_K(\mathbf{r})=\mathbf{N}\cdot\mathbf{r}g(2i\psi_K)\gamma\cdot\mathfrak{P}_K e^{i\mathbf{K}\cdot\mathbf{r}}e^{-\alpha_1\mathbf{N}\cdot\mathbf{r}}, \quad (5.25)$$

with ψ_K given by (5.24).

[15] J. A. Stratton, *Electromagnetic Theory* (McGraw-Hill Book Company, Inc., New York, 1941), Sec. 9.13.

5.3 Expansion of the Mismatch Function

Before (5.25) can be applied it is necessary to express the mismatch function φ' of (5.24) and (5.11) in terms of the components of $\mathbf{K}$. It is convenient to define the vectors

$$\boldsymbol{\eta}=(c/\omega)\mathbf{K}=n'\boldsymbol{\sigma},\quad \boldsymbol{\eta}_1=(c/\omega)2\mathbf{k}_1,\quad \boldsymbol{\eta}_2=n_2(\mathbf{s})\mathbf{s}. \tag{5.26}$$

The vector $\boldsymbol{\eta}_2$ is constrained to lie on the index surface for the second harmonic shown in Fig. 2; the vector $\boldsymbol{\eta}_1$ lies on this index surface in the matching direction; the vector $\boldsymbol{\eta}$ is arbitrary, and we are required to find φ' as a function of η. The mismatch equation (5.11) becomes in the notation of (5.26)

$$\boldsymbol{\eta}-\boldsymbol{\eta}_2=\varphi'\mathbf{N}. \tag{5.27}$$

We shall assume that the surface normal $\mathbf{N}$ is a matching direction, and also that $\boldsymbol{\eta}_1$ is in the direction $\mathbf{N}$.

The relation (5.27) is shown geometrically in Fig. 8. As in Fig. 2 we have taken the z direction to be along $\mathbf{N}$, the optic axis in the xz plane, and the y directional normal to the plane of the figure. The tangent plane to the index surface at $\boldsymbol{\eta}_1$ is shown, and the normal to this plane makes the angle ρ with $\mathbf{N}$. The mismatch φ' according to (5.27) is the distance from $\boldsymbol{\eta}$ to the index surface measured parallel to $\mathbf{N}$. This may be written as an expansion in powers of the components of $(\boldsymbol{\eta}-\boldsymbol{\eta}_1)$ as follows

$$\varphi'(\boldsymbol{\eta})=\varphi'^{(1)}+\varphi'^{(2)}+\cdots, \tag{5.28}$$

where $\varphi'^{(1)}$ is linear and $\varphi'^{(2)}$ is quadratic, etc. In Fig. 8 $\varphi'^{(1)}$ is shown as the distance from $\boldsymbol{\eta}$ to the tangent plane.

The equation in $\boldsymbol{\eta}$ space for the tangent plane is

$$\eta_z-n+\eta_x\tan\rho=0. \tag{5.29}$$

It follows that $\varphi'^{(1)}$ is given by

$$\varphi'^{(1)}=\eta_z-n+\eta_x\tan\rho, \tag{5.30}$$

where n is the (matched) refractive index. To the second order in $(\boldsymbol{\eta}-\boldsymbol{\eta}_1)$, $\varphi'^{(2)}$ is the distance in $\boldsymbol{\eta}$ space from the tangent plane to the index surface measured on a line through $\boldsymbol{\eta}$ parallel to $\mathbf{N}$. For a uniaxial crystal the index surface is an ellipsoid of revolution; corresponding to a negative uniaxial crystal like ADP we shall put the semimajor axis equal to $n_2{}^o$ and the semiminor axis equal to $n_2{}^e$. It is somewhat tedious but elementary to show that

$$\varphi'^{(2)}=\tfrac{1}{2}n[(n\eta_x/n_2{}^on_2{}^e)^2+(\eta_y/n_2{}^e)^2]. \tag{5.31}$$

Since $\varphi'^{(2)}$ is a small correction to $\varphi'^{(1)}$, and the crystal will usually be nearly isotropic, it is proper to replace (5.31) by the simpler relation

$$\varphi'^{(2)}=(\eta_x{}^2+\eta_y{}^2)/2n. \tag{5.32}$$

It now follows from (5.24) that $2\psi_K$ can be written

$$2\psi_K=(K_z-2k_1+\rho K_x)z+i\alpha z+[(K_x{}^2+K_y{}^2)/4k_1]z \tag{5.33}$$

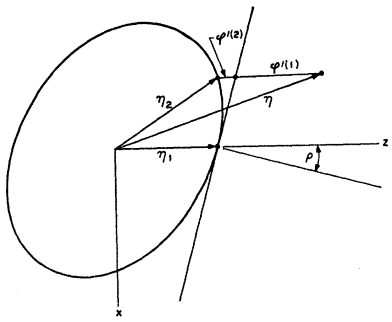

FIG. 8. Geometrical representation of the mismatch relation (5.27). The surface normal is in the z-direction, and the index surface, tangent plane, and ρ line are the same as in Fig. 2.

to the second order in the components of $\mathbf{K}-2\mathbf{k}_1$. We have set $\tan\rho=\rho$ since $\rho\ll1$.

5.4 Representation of the Polarization

The polarization $\mathfrak{P}(\mathbf{r})$ produced in the crystal by the laser beam will not be an unbounded plane wave of the form assumed on the right side of (5.5), although for some purposes this may be an adequate approximation. The beam will in general be finite in aperture, and therefore requires many Fourier components to represent it. We shall represent the polarization beam by the Fourier integral

$$\mathfrak{P}(\mathbf{r})=\exp(-\alpha_1\mathbf{N}\cdot\mathbf{r})\int\mathfrak{P}_K e^{i\mathbf{K}\cdot\mathbf{r}}d\mathbf{K} \tag{5.34}$$

over the three components of $\mathbf{K}$. We have written the effect of absorption as a separate factor rather than include it in $\mathfrak{P}_K$. It follows that

$$\int\mathfrak{P}_K e^{i\mathbf{K}\cdot\mathbf{r}}d\mathbf{K}=\mathfrak{P}(\mathbf{r})_{NA} \tag{5.35}$$

represents the polarization with *no absorption* of the laser beam. The inversion of (5.35) is

$$\mathfrak{P}_K=(2\pi)^{-3}\int\mathfrak{P}(\mathbf{r})_{NA}e^{-i\mathbf{K}\cdot\mathbf{r}}d\mathbf{r}. \tag{5.36}$$

The integral is to be taken over all space where $\mathfrak{P}(\mathbf{r})_{NA}$ is different from zero. We let $z=0$ be the incident surface and $z=\ell$ the exit surface of the crystal; we then have

$$\mathfrak{P}(\mathbf{r})_{NA}=0\qquad z<0,\ z>\ell. \tag{5.37}$$

The convergence of (5.36) as $\ell\to\infty$ is assured by the fact that $\mathfrak{P}(\mathbf{r})_{NA}$ must fall off as z^{-2} at distances large compared to the beam aperture.

We shall assume that the Fourier components $\mathfrak{P}_K$ are very small except in a small neighborhood of $\mathbf{K}$ space containing $2\mathbf{k}_1$. Here $\mathbf{k}_1$ is the nominal wave

vector of the laser beam, the wave vector we would use were we to represent the laser beam by a single plane wave. We also assume that $\mathbf{K}=2\mathbf{k}_1$ is a matched wave vector. The beam also contains components $\mathbf{K}$ which are mismatched which give rise to all the specific effects of the finite aperture.

Each plane-wave component of (5.34) produces its own second-harmonic electric field given by (5.25). The resultant second-harmonic field can be written

$$\mathbf{E}_2(\mathbf{r})=ze^{-\alpha_1 z}\int_0^1 dp\int\gamma\cdot\mathfrak{P}_K e^{-2ip\psi_K}e^{i\mathbf{K}\cdot\mathbf{r}}d\mathbf{K}, \quad (5.38)$$

where use has been made of the integral representation in (5.13), and we have set $\mathbf{N}\cdot\mathbf{r}=z$. This together with the representation of ψ_K in (5.33) and the definition of $\mathfrak{P}_K$ in (5.36) is our basic equation.

5.5 Mixing

It should be emphasized that (5.38) takes into account all the contributions from mixing the different Fourier components of the laser beam. Let the laser beam $\mathbf{E}_1(\mathbf{r})$ be represented as a Fourier integral

$$\mathbf{E}_1(\mathbf{r})=e^{-\alpha_1 z/2}\int\mathbf{E}_k e^{i\mathbf{k}\cdot\mathbf{r}}d\mathbf{k}. \quad (5.39)$$

The polarization is given by[2]

$$\mathfrak{P}(\mathbf{r})=d\cdot\mathbf{E}_1(\mathbf{r})\mathbf{E}_1(\mathbf{r}), \quad (5.40)$$

where d is the second-order polarization tensor. Thus

$$\begin{aligned}\mathfrak{P}(\mathbf{r})&=e^{-\alpha_1 z}\int\int d\cdot\mathbf{E}_k\mathbf{E}_{k'}e^{i(\mathbf{k}+\mathbf{k}')\cdot\mathbf{r}}d\mathbf{k}d\mathbf{k}'\\&=e^{-\alpha_1 z}d\cdot\int d\mathbf{K}e^{i\mathbf{K}\cdot\mathbf{r}}\int d\mathbf{k}\mathbf{E}_k\mathbf{E}_{K-k}.\end{aligned} \quad (5.41)$$

It now follows from (5.34) that the Fourier components of the polarization are related to those of the fundamental beam by the integral

$$\mathfrak{P}_K=d\cdot\int d\mathbf{k}\mathbf{E}_k\mathbf{E}_{K-k}. \quad (5.42)$$

This expresses the *mixing property* of the second-order polarization.

The components $\mathbf{E}_k$ can be found from

$$\mathbf{E}_k=(2\pi)^{-3}\int\mathbf{E}_1(\mathbf{r})_{NA}e^{-i\mathbf{k}\cdot\mathbf{r}}d\mathbf{r}, \quad (5.43)$$

where $\mathbf{E}_1(\mathbf{r})_{NA}$ is the laser field with *no absorption*. Under favorable experimental conditions (single-mode laser operation) $\mathbf{E}_1(\mathbf{r})_{NA}$ will be precisely known from confocal-resonator theory.[5,6] Thus $\mathbf{E}_k$ can be determined from (5.43) and then $\mathfrak{P}_K$ can be determined from the mixing relation (5.42). It is more convenient in practice, however, to compute $\mathfrak{P}_K$ directly from the integral

$$\mathfrak{P}_K=(2\pi)^{-3}\int d\cdot\mathbf{E}_1(r)_{NA}\mathbf{E}_1(\mathbf{r})_{NA}e^{-i\mathbf{K}\cdot\mathbf{r}}d\mathbf{r}, \quad (5.44)$$

which is just a more detailed way of writing (5.36).

5.6 Double Refraction for Parallel Beams

Double refraction can be elucidated by means of an idealization which eliminates the complications arising from diffraction. In this section we shall consider SHG by idealized *parallel beams* of the form

$$\mathfrak{P}(\mathbf{r})=e^{-\alpha_1 z}e^{2ik_1 z}\mathfrak{P}(x,y)B(z), \quad (5.45)$$

where $\mathfrak{P}(x,y)$ is independent of z, and $B(z)$ represents a slab of thickness ℓ

$$\begin{aligned}B(z)&=0(z<0)\\&=1(0\leq z\leq\ell)\\&=0(z>\ell).\end{aligned} \quad (5.46)$$

The best example of a parallel beam is a laser beam in the fundamental mode of a confocal resonator. Some of the properties of these modes have been reviewed in Sec. 2. Even in this case, however, the beam can only be considered parallel in the *near field*,

$$\xi\ll 1, \quad (5.47)$$

where ξ has been defined in (2.4).

5.6.1 Basic Theory

It will be shown later that as a consequence of the near field approximation (or the parallel assumption) the quadratic terms of (5.33) can be neglected. It then follows from (5.38) and (5.36) that

$$\begin{aligned}\mathbf{E}_2(x,y,z)=ze^{-\alpha_1 z}\int_0^1 dpe^{p\alpha z}\int d\mathbf{K}e^{i\mathbf{K}\cdot\mathbf{r}}e^{-ipz(K_z-2k_1+\rho K_x)}\\\times(2\pi)^{-3}\int d\mathbf{r}'\gamma\cdot\mathfrak{P}(x',y')B(z')e^{2ik_1 z'}e^{-i\mathbf{K}\cdot\mathbf{r}'}.\end{aligned} \quad (5.48)$$

The integration over $\mathbf{K}$ gives the factor

$$(2\pi)^3\delta(x-x'-p\rho z)\delta(y-y')\delta(z-z'-pz). \quad (5.49)$$

If we assume that z lies in the active slab $0\leq z\leq\ell$ the integration over $\mathbf{r}'$ gives

$$\mathbf{E}_2(x,y,z)=ze^{-\alpha_1 z}e^{2ik_1 z}\int_0^1 dpe^{p\alpha z}\gamma\cdot\mathfrak{P}(x-p\rho z,y), \quad (5.50)$$

which is the desired result.

The same result is obtained if the slab function $B(z)$ is omitted from (5.45), except that we would then not

restrict z to the region $z\leq\ell$. Thus, if z is restricted to the slab, the values of $\mathfrak{P}(x,y,z)$ outside the slab are immaterial.

According to (5.50) the field at the exit surface of the crystal can be written (dropping the unimportant factor $e^{2ik_1\ell}$)

$$\mathbf{E}_2(x,y,\ell)=e^{-\frac{1}{2}\alpha_2\ell}\int_0^\ell dze^{-\alpha z}\gamma\cdot\mathfrak{P}(x-\rho\ell+\rho z,\, y)\,, \quad (5.51)$$

where now z is a dummy variable of integration $z=(1-p)\ell$ replacing p in (5.50). This result is identical with (3.11) of the heuristic treatment. A detailed discussion of *double refraction* based on this equation has been given in Sec. 3 for the case in which the laser beam is in the fundamental mode. The experimental confirmation of the results derived from (5.51) has been presented in Sec. 4. The derivation given in this paragraph confirms the validity of the heuristic method for the near field. From our heuristic discussion we know that the variable z in (5.51) can be interpreted in accordance with our usual notation as the distance from the incident surface. The integral can be interpreted as a summation over the contributions of the dipoles in the slab to the field at the exit surface.

5.6.2 *Fourier Method*

We have obtained our result (5.50) without explicitly considering the Fourier components $\mathfrak{P}_K$. The same result can be obtained in any specific case by the Fourier method. From (5.36) and (5.45)

$$\mathfrak{P}_K=(2\pi)^{-2}\int\int dxdy\mathfrak{P}(x,y)e^{-iK_xx-iK_yy}$$
$$\times(2\pi)^{-1}\int dzB(z)e^{i(2k_1-K_z)z}. \quad (5.52)$$

If the laser beam is in the fundamental mode (2.1), $\mathfrak{P}(x,y)$ is of the form

$$\mathfrak{P}(x,y)=\mathfrak{P}_0e^{-2(x^2+y^2)/w_0^2}. \quad (5.53)$$

As discussed above it is permissible to omit $B(z)$ providing we consider points z not outside the slab. The evaluation of (5.52) then gives

$$\mathfrak{P}_K=\mathfrak{P}_0(w_0^2/8\pi)\delta(2k_1-K_z)e^{-w_0^2(K_x^2+K_y^2)/8}. \quad (5.54)$$

Inserting (5.54) into (5.38) and retaining only the linear terms of (5.33) gives

$$\mathbf{E}_2(x,y,z)=z\gamma\cdot\mathfrak{P}_0e^{-\alpha_1z}e^{2ik_1z}$$
$$\times\int_0^1 dpe^{p\alpha z}e^{-2[y^2+(x-p\rho z)^2]/w_0^2}, \quad (5.55)$$

which also agrees with (5.50) and (3.16). Although it is unnecessary in practice to evaluate $\mathfrak{P}_K$, since the Fourier method must always agree with the general result (5.50) in the case of a parallel beam, the Fourier method is of practical importance when diffraction effects are to be taken into account.

The validity of neglecting the quadratic terms of (5.33) is a consequence of the small magnitude of these terms compared with the quadratic terms in the exponent of (5.54). If we retain the quadratic terms, (5.38) contains the factor

$$\exp\{-(K_x^2+K_y^2)[\tfrac{1}{8}w_0^2+i(pz/4k_1)]\}\,, \quad (5.56)$$

with the second term in the exponent coming from (5.33). Since $p\leq1$ the condition for the dropping of this term is

$$z/4k_1\ll w_0^2/8\,, \quad (5.57)$$

which is identical with the near-field criterion (5.47). This confirms the validity of the linear approximation for ψ_K for parallel beams.

Here we have applied the formal theory to the case of SHG in the near field where the polarization beam may be considered parallel. The method based upon (5.38) is quite general, however, and will be applied in a subsequent paper to the far field where diffraction effects play a dominant role.

6. SUMMARY

We have presented a discussion of the effects of double refraction and absorption on the second-harmonic generation of light under index-matching conditions, treating the negative uniaxial crystal in detail. In Sec. 2 we have described experiments in which the second-harmonic intensity distribution was measured by means of a detector equipped with a traveling slit. The second-harmonic beam was generated in long crystals of ADP by an essentially parallel beam from a gas laser in single-mode operation. It was found, as described in Sec. 2, that the peak of the second-harmonic beam is displaced a few millimeters from the center of the laser beam. This is the first reported observation of this effect, which had previously been predicted and called the aperture effect, since its observation depends upon the displacement being larger than the beam aperture. A characteristic length, the aperture length, has been defined which measures the crystal length at which the aperture effect begins to limit the second-harmonic power.

In order to discuss the experiments in the simplest possible way we have given a heuristic theory in Sec. 3 which makes use of several *ad hoc* but plausible assumptions. This theory starts with the familiar theory of SHG by unbounded plane waves. The finite intensity distribution of the fundamental (laser) beam and the correct direction of energy propagation of the second harmonic are then inserted into an integral expression for the second-harmonic field. Results are obtained for the intensity distribution of the second harmonic.

It is found that an effect occurs in SHG that is closely related to the familiar phenomenon of double refraction. In double refraction parallel light from a slit entering the crystal will split into two beams and emerge from the crystal as two separate parallel beams. In SHG double refraction causes the second-harmonic intensity to spread uniformly over the region that lies between the two beams of ordinary double refraction. This uniform spreading of intensity only applies to the case of no absorption. In the presence of absorption the second-harmonic intensity peaks somewhere between the double-refraction beams depending on the relative absorptions of the laser and second harmonic. This is the aperture effect.

In Sec. 4 the experimental data is compared quantitatively with the theory in regard to the position of the peak, the shape of the intensity distribution, and the dependence of peak intensity and total power on spot size of the laser beam. The theory was found to be in satisfactory agreement with experiment.

In Sec. 5 a formal treatment is given based upon a Fourier representation of the polarization beam. It is shown that this treatment properly includes all mixing effects. Double refraction is obtained from the formal theory by considering an idealized parallel beam. Such a beam is a reasonable approximation for the laser beam in the near field. The formal treatment gives in this case the same result as the heuristic treatment; this confirms the validity of the latter for parallel beams.

The investigations reported here, experimental and theoretical, have filled in several gaps that previously existed in the literature of nonlinear optics. Specifically, we have: (a) experimentally studied SHG in very long crystals ($\sim$10 cm) with essentially parallel gas laser beams in order to determine the limits over which coherence can be maintained; (b) experimentally observed and measured the aperture effect (double refraction); (c) given a simple heuristic theory for the beam shape in double refraction; (d) shown that the theory and experiment are in good quantitative agreement; (e) presented a rigorous theory for SHG under matching conditions which does not require the *ad hoc* assumptions of the heuristic theory; (f) verified the correctness of the heuristic theory for parallel beams.

ACKNOWLEDGMENTS

Our thanks to W. L. Bond, for resurrecting the very large ADP crystals used herein, and Mrs. C. A. Lambert for the numerical treatment of the functions involved. W. Pleibel most ably prepared the samples.

APPENDIX

We shall now show formally that the Poynting vector (averaged over time)

$$\mathbf{S}=(c/8\pi)\mathbf{E}\times\mathbf{H}^* \tag{A.1}$$

for a plane wave of the form (5.6)

$$\mathbf{E}(\mathbf{r})=E\mathbf{U}e^{i(\omega/c)n\mathbf{s}\cdot\mathbf{r}} \tag{A.2}$$

is in the direction of the normal to the index surface at $\mathbf{s}$ as shown in Fig. 2. A detailed formal treatment of this problem has been given by Kogelnik and Motz,[12] but we shall use a simpler method similar to that of Born and Wolf.[16] Born and Wolf do not consider the index surface, which is the reason we include this Appendix.

The equation satisfied by the unit vector $\mathbf{U}$ according to (5.8) and (5.9) may be written

$$\epsilon\cdot\mathbf{U}=\boldsymbol{\eta}\cdot\boldsymbol{\eta}\mathbf{U}-\boldsymbol{\eta}(\boldsymbol{\eta}\cdot\mathbf{U}), \tag{A.3}$$

where $\boldsymbol{\eta}$ is the refractive index vector

$$\boldsymbol{\eta}=n\mathbf{s} \tag{A.4}$$

first used in (5.26). The tangent plane to the index surface may be defined as the locus of all vectors $\delta\boldsymbol{\eta}$ for arbitrary (small) variations $\delta\mathbf{s}$. Thus any vector which satisfies

$$\delta\boldsymbol{\eta}\cdot\mathbf{S}=0 \tag{A.5}$$

for all $\delta\boldsymbol{\eta}$ must be normal to the index surface; this is the key point in the proof. Now take the variation of (A.3); by multiplying on the left by $\mathbf{U}$ and invoking the symmetry of the ϵ tensor

$$\mathbf{U}\cdot\epsilon=\epsilon\cdot\mathbf{U} \tag{A.6}$$

one obtains

$$\delta\boldsymbol{\eta}\cdot[\boldsymbol{\eta}-(\boldsymbol{\eta}\cdot\mathbf{U})\mathbf{U}]=0. \tag{A.7}$$

The magnetic field $\mathbf{H}(\mathbf{r})$ is given by

$$\begin{aligned}\mathbf{H}(\mathbf{r})&=-(ic/\omega)\nabla\times\mathbf{E}(\mathbf{r})\\&=nE\mathbf{s}\times\mathbf{U}e^{i(\omega/c)n\mathbf{s}\cdot\mathbf{r}}.\end{aligned} \tag{A.8}$$

It follows that the Poynting vector $\mathbf{S}$ can be written

$$\mathbf{S}=-(nc/8\pi)|E|^2[\mathbf{U}(\mathbf{s}\cdot\mathbf{U})-\mathbf{s}], \tag{A.9}$$

and it further follows from (A.7) that $\mathbf{S}$ satisfies (A.5). This completes the proof.

---

[16] M. Born and E. Wolf, *Principles of Optics* (Pergamon Press, Inc., London, 1959), Sec. 14.2.3.